Three-Dimensional Reconstruction of Fibrin Clot Networks from Stereoscopic Intermediate Voltage Electron Microscope Images and Analysis of Branching

Timothy C. Baradet, *John C. Haselgrove,‡ and John W. Weisel*

*Department of Cell and Developmental Biology, University of Pennsylvania School of Medicine, Philadelphia, Pennsylvania 19104, and ‡Department of Radiology, Children's Hospital of Philadelphia, Philadelphia, Pennsylvania 19104 USA

ABSTRACT Fibrin polymerizes to produce branching fibers forming a three-dimensional network, which has been difficult to visualize by conventional microscopy. Three-dimensional images of whole clots at high resolution were obtained from stereo-pair intermediate-voltage electron micrographs. Computer software was developed to produce three-dimensional reconstructions of the networks in the form of a pattern of links that connect branching junctions. Network parameters were measured and analyzed to characterize the clots quantitatively. Models in which all links were moved to the origin, while preserving their orientation, allowed visualization of some network parameters and facilitated comparison of networks. Fibrin clots formed in three different conditions were analyzed and compared by these methods. Clots formed in 0.20 M saline buffer consist of fibers of uniform size, and most of the branching junctions consist of three links. Fibrin clots formed in 0.05 M saline buffer are made up of very large diameter fiber bundles with far fewer branching junctions and correspondingly longer links. Clots formed in 0.40 M saline buffer consist of very fine fibers with numerous branching junctions and very short links. In summary, the extent of lateral aggregation is directly related to the distance between branching junctions and inversely related to the total number of branching junctions. These observations must be considered in defining possible mechanisms of fibrin branching.

INTRODUCTION

The formation of fibrin blood clots from fibrinogen has been extensively studied by biochemical and biophysical methods. The clot assembly process consists of several distinct steps, each affecting the rate of fibrin fiber assembly and the spatial arrangement of fibers in the completed clot. The first important step is the cleavage of a pair of A fibrinopeptides from the fibrinogen molecule by the serine protease, thrombin. Once the fibronopeptides are released, binding sites are exposed in the central domain that are complementary to sites at the ends of the fibrin monomers. These bind in a half-staggered manner to form dimers, and small oligomers grow to yield protofibrils (Fowler et al., 1981). The subsequent cleavage of B fibrinopeptides by thrombin exposes additional binding sites and promotes lateral aggregation. Further extension and lateral aggregation of protofibrils results in fibrin fibers and complete clot networks (Erickson and Fowler, 1983; Medved et al., 1990).

Experiments using spectrophotometric methods to study fibrinogen to fibrin conversion followed by fibrin monomer aggregation have demonstrated an inverse relationship between ionic strength and clot turbidity. An increase in the molarity of the clot formation environment causes a decrease in absorbance at 350 nm (Ferry and Morrison, 1947; Latallo et al., 1962; Hantgan and Hermans, 1979; Hantgan et al., 1980). The effect of calcium ions on the clotting process has also been widely documented (Hardy et al., 1983; Carr et al., 1986). Other experiments have correlated the effects of clotting time, fibrin concentration, ionic strength, pH, and fibrinopeptide release on turbidity with the permeability to liquid of the resultant clots (Blombäck and Masahisa, 1982).

Early investigations of fibrin clot structures using transmission electron microscopy first revealed some aspects of fiber morphology and clot structure (Hawn and Porter, 1947). Clots formed under various ionic conditions showed dramatic differences in structure. Since then, a wide variety of studies by transmission electron microscopy has provided extensive information about the structure of supramolecular assemblies at different stages of polymerization. Some of these studies have established the significance of the two pairs of fibrinopeptides and their relationship to the lateral aggregation of fibrin fiber assemblies in clot formation (Weisel, 1986) as well as the role of fiber twisting (Weisel et al., 1987). The formation of small fibrin aggregates and protofibrils has also been studied using transmission electron microscopy (Medved' et al., 1990). Several factors appear to play important roles in determining the final fiber diameter and clot structure, and all are greatly affected by the kinetics of each individual step (Medved' et al., 1990; Mosesson et al., 1987; Langer et al., 1988).

High-voltage electron microscopy has been used previously to study clot structures of both normal fibrinogen and fibrinogen Metz, an abnormal human fibrinogen with the amino acid substitution $A\alpha_{16}$ Arg → Cys (Mosesson et al., 1987). This study used stereo-pair electron micrographs but was limited to relatively thin specimens. Fiber diameters were measured, but these images were very complex and would be difficult to analyze further. Fibrin films and fine

Received for publication 6 June 1994 and in final form 13 December 1994.

Address reprint requests to John W. Weisel, Department of Cell and Developmental Biology, University of Pennsylvania School of Medicine, Philadelphia, PA 19104-6058. Tel.: 215-898-3573; Fax: 215-898-9871; E-mail: weisel@anat3d2.anatomy.upenn.edu.

0006-3495/95/04/1551/10 $2.00

fibrin clots produced at high ionic strength have also been studied with high-voltage instruments (Müller et al., 1984).

Ultrastructural studies by scanning electron microscopy can yield significant data, especially with respect to the surface features of clots, but are limited in the depth of visualization (Weisel and Nagaswami, 1992). The effect of deglycosylation on fibrin fiber formation has been studied utilizing both scanning and transmission electron microscopy (Langer et al., 1988). A scanning electron microscope study correlated computer models of the kinetics of polymerization to clot morphology (Weisel and Nagaswami, 1992).

We have examined clots by intermediate voltage electron microscopy (IVEM) and developed computer software to analyze the three-dimensional network structures using stereo pairs. IVEM allows for the observation of specimens almost as thick as those prepared for either scanning electron microscopy or high-voltage electron microscopy. IVEM images offer greater resolution than scanning electron microscope images, and deeper clot structures are not obscured by surface features. Tilting of the specimen to produce stereo pairs yields information about the third dimension. Through the use of a customizable image analysis program, the fibrin clots can be analyzed in three dimensions to obtain morphometric parameters such as fiber diameter, distance between branching points of fibers, and branching complexity. By using other programs, a three-dimensional "wire-frame" model of a clot can be generated. This model can be rotated and zoomed to observe clot fiber relationships from perspectives not available by use of the raw data alone. This system was developed specifically in an attempt to quantify the changes in fibrin fiber clot structures that result from differences in environmental conditions. The observations made here correlate well with previous data on clot formation and yield insights into mechanisms of clot assembly and fiber branching.

MATERIALS AND METHODS

Specimen preparation for electron microscopy

Solutions of purified human fibrinogen at a concentration of 0.5 mg/mL in 0.40 M, 0.20 M, and 0.05 M NaCl buffers with 0.05 M Tris-HCl, pH 7.4, and 2 mM $CaCl_2$ were used for these experiments. Fibrinogen solutions were mixed with thrombin to a final concentration of 0.3 U/mL and aliquots placed onto Formvar and carbon-coated grids. After clotting for 1 h at room temperature, clots were fixed with 3% glutaraldehyde in 0.1 M sodium-cacodylate buffer, pH 7.2, for 5 min. Grids were kept constantly moist to avoid collapse or syneresis. Clots were washed 3 times in the same buffer and stained *en bloc* with saturated aqueous uranyl acetate for 2 min. After staining, they were transferred to a custom-built grid holder, rinsed 3 times in distilled water, and dehydrated in graded ethanol. Following dehydration, the clots were critical-point dried from CO_2. As a result of the observation of electron beam damage in test grids, experimental samples were subsequently rotary carbon coated using a Denton DV-502 vacuum evaporator (Denton Vacuum Corp., Cherry Hill, NJ), at a vacuum $<10^{-6}$ torr.

Electron microscopy and production of stereo pairs using IVEM

The prepared clots were examined in a JEOL JEM-4000 EX transmission electron microscope at 400 kV (JEOL Ltd., Tokyo, Japan). Stereo pairs were taken at angles of 0°, ±2°, and ±5° using a tilting, eucentric goniometer stage on the microscope. The tilt stage and the specimen holder were a custom-designed modification of the standard equipment.

Electron micrographs were digitized for image analysis using a Videk Megaplus CCD camera (Eastman-Kodak, Inc., Rochester, NY). This camera is a frame-transfer type capable of producing a 1024 × 1280 pixel image. The camera was controlled by custom control/acquisition software, and images were acquired via a digital frame capture board mounted in a desktop computer.

Image analysis software for three-dimensional model building and analysis

Stereo-pair images were ported to the image analysis system, which consists of a Silicon Graphics Indigo XS-24Z workstation with a 1024 × 1280 pixel, 24-bit color monitor (Silicon Graphics Inc., Mountain View, CA.). Custom image analysis software routines were written in IDL (Interactive Data Language, RSI Systems, Boulder, CO). Clot fiber measurements and three-dimensional data sets for wire-frame models were generated using this system combined with an optical stereo viewer. Stereo-pair wire-frame models and "sea-urchin" models were observed and edited using original software. This program allows full rotation of the clot wire-frame model on all three axes with both image zoom and data point identification functions.

RESULTS

Three-dimensional reconstruction of fibrin networks

Clots were formed under three different buffer conditions and samples of each prepared for viewing in the intermediate voltage electron microscope. While the higher accelerating voltages allowed the electron beam to penetrate and image a specimen of whole clot, the resulting micrographs (Fig. 1) were possibly even more difficult to interpret than scanning electron micrographs. Instead of an image of the surfaces of fibers at different depths, one sees a projection of all layers of fibers. Tilting the specimen to produce stereo pairs allowed the visualization of the specimen in three dimensions, so that individual fibers could be followed and their connections studied (Fig. 1).

In viewing these stereo pairs, it quickly became apparent that most of the networks were too complex to be comprehended and analyzed readily by visual inspection. Computer software was developed so that the networks could be visualized more easily, different views could be obtained, and the networks analyzed quantitatively.

The resultant software package provides methodology for the three-dimensional reconstruction of clot fiber networks. Stereo-pair images of specimens suitable for analysis were digitized (Fig. 2 *A*). The stereo pairs were displayed on the computer monitor and aligned for viewing in stereo with an optical viewer. The branching junctions were then marked with a cursor that can be moved along all three axes (x, y, and z) (Fig. 2 *B*). Links or fiber segments that connect branching junctions were also marked (Fig. 2 *C*). We use the term "links" because the structures making up the network can be either fibers or fiber bundles. By repeating these procedures, the entire clot network was reconstructed. The software also allows for editing of the points used in the reconstruction to correct errors. By continually comparing the reconstruction with the original digitized stereo pairs, it is

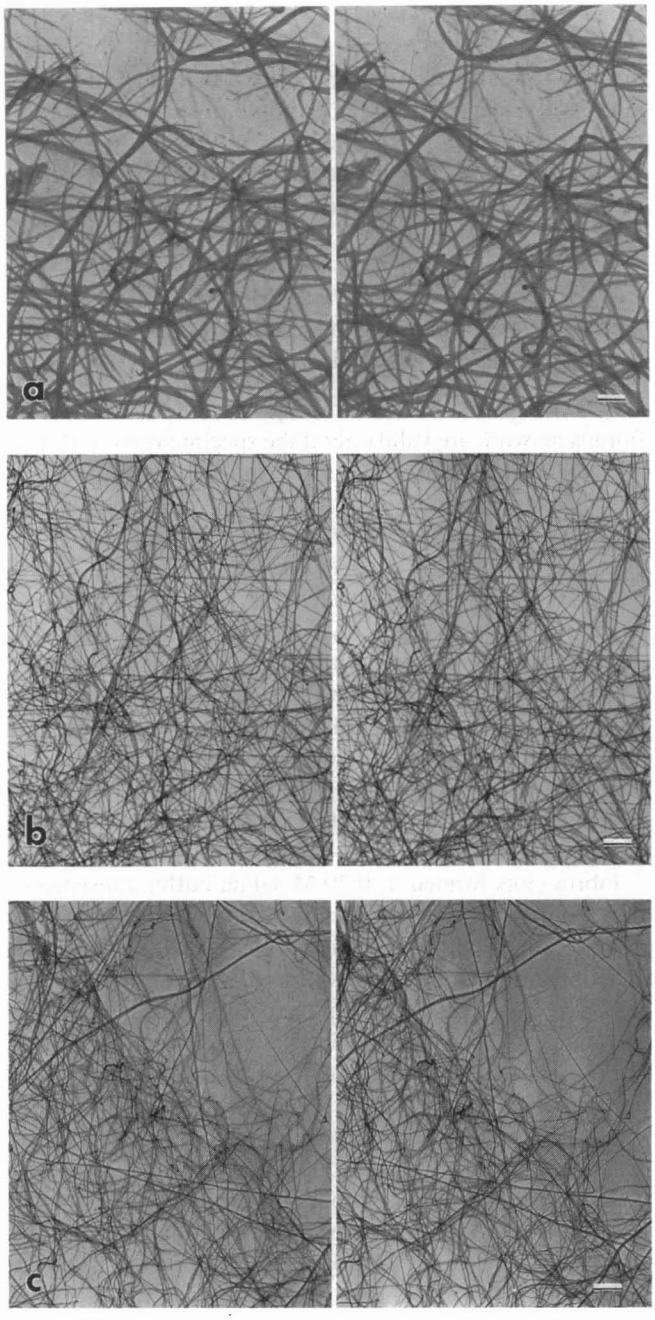

FIGURE 1 Stereo-pair images of intermediate-voltage (400 kV) electron micrographs of fibrin clots formed under three different ionic conditions. (*A*) Stereo pair of clot formed in 0.05 M ionic strength buffer. (*B*) Stereo pair of clot formed in 0.20 M ionic strength buffer. (*C*) Stereo pair of clot formed in 0.40 M ionic strength buffer. Bar = 500 nm.

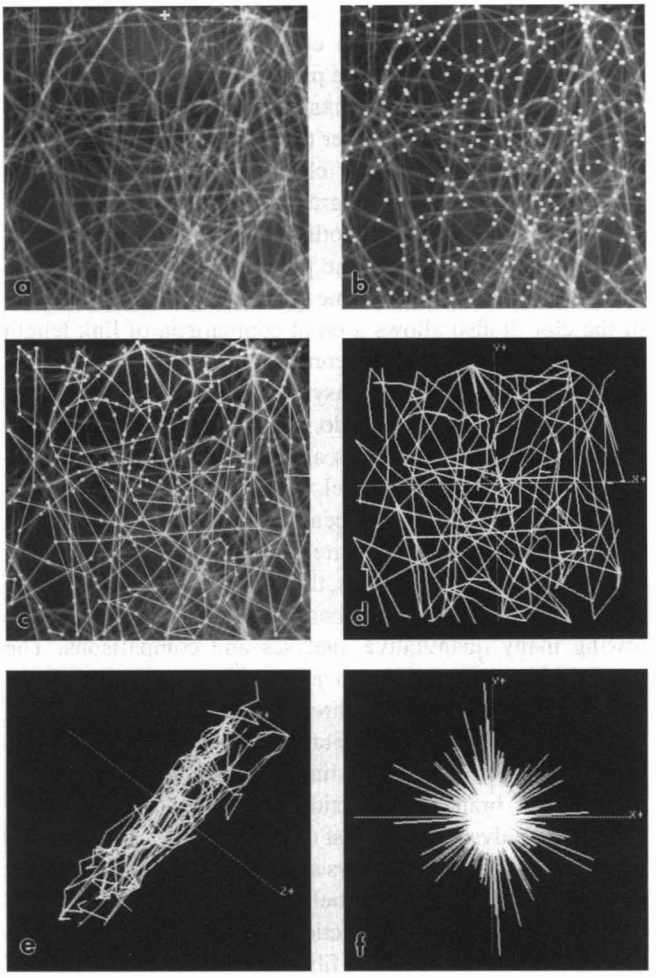

FIGURE 2 Outline of the process for building three-dimensional computer reconstructions from stereo-pair electron micrographs of a clot formed in 0.20 M ionic strength buffer. (Nonstereo images taken from the computer monitor are shown here.) (*A*) Digitized electron micrograph of clot formed in 0.20 M ionic strength buffer. (*B*) Digitized electron micrograph overlaid with square markers for branching junctions placed in three dimensions by viewing the images in stereo. (*C*) Previous image with the addition of the white lines representing the connecting links between branching junctions in three-dimensions. (*D*) Completed three-dimensional model built from branching junction markers and connecting links, without the digitized image from which it was derived. (*E*) Model rotated to show unique view from the side; this clot is ~0.9 μm thick. (*F*) Model shown as a "sea-urchin" representation, which is formed by moving the branching link vectors to the origin while retaining their angular orientation. In effect, this representation is a three-dimensional polar coordinate plot showing the distribution and orientation of the length of the links between branching junctions.

possible to build accurate models. The reconstructions can also be displayed independently of the original micrographs (Fig. 2 *D*).

The three-dimensional reconstruction also allows unique views of the clots. The reconstruction can be rotated around all three axes for viewing at any angle (Fig. 2 *E*). The capability of model rotation permits views that would not be possible by electron microscopy. The depth and complexity of the modeled clot can be observed from a lateral view, and models can be rotated and "zoomed" to study details of fiber interactions. As the model is rotated and the viewpoint changes, the rotational coordinates can be displayed. In addition, the identification of any branching junction is possible. These features are invaluable in the process of model building by allowing rapid identification of inaccurate point selections and branching junctions that have been linked incorrectly.

An additional feature is the generation of a unique three-dimensional model representing the length and orientation of each of the branching junction links in the reconstructed clot. By translating the end of each link to the origin of a three-dimensional set of axes, while retaining the angular orien-

tation of each link, a model that resembles a sea urchin can be generated (Fig. 2 *F*). In effect, this model is a three-dimensional polar coordinate plot of link length distribution and orientation. Since the links have no polarity, there is no reason to choose one end over the other for placement at the origin. Because an arbitrary choice could introduce asymmetry into the sea urchin diagrams, all the links at each node were placed at the origin. In other words, each link is doubly represented but with opposite polarity. This model may be rotated and zoomed in the same manner as the skeleton model of the clot. It also allows a rapid comparison of link length and distribution among different clot specimens, as well as rapid identification of any asymmetry or inhomogeneities. These "sea urchin" models do not require a separate reconstruction process; the values are computed from data generated by the skeleton model, and the software allows instantaneous switching between the two types of model.

The reconstruction software records all variables of the clot structures traced (lengths, three-dimensional coordinates of branching junctions, number links of connected, etc.), allowing many quantitative analyses and comparisons. The mean link length and the mean angular orientation of the links can be determined in three dimensions. Link diameter can be measured at any orientation. Mean distance between branch points (link lengths), link diameters, and the number of links per branching junction were measured using the computer analysis system just described (Table 1). The size distributions of link diameters and lengths are plotted in Fig. 4 and the results described below.

In general, the reconstructions represent very accurate models of clot structures and fiber interactions (Fig. 3). Models of clot fiber networks were built using the computer analysis system and compared with photographic prints of stereo pairs to assess the accuracy of the models. The arrangement of fibers and the branching pattern can be easily seen. The distances between branching junctions and the angles of the links at the branching junctions are more easily visualized than in the original micrographs. The spacing between fibers, or "porosity," of the clot can also be observed.

There are a few exceptions to the accuracy of the reconstructions. In some cases, a comparison of prints with digitized images demonstrated a loss of fine detail, although this is not intrinsic to the system. The significance of the digitizing conditions for images of clots formed in 0.40 M saline buffer will be discussed later. Stereo-pair IVEM images of clots may be compared in Fig. 1, while stereo-pair models of reconstructed clots may be compared in Fig. 3. In addition, the model does not allow an accurate depiction of differences in the diameters of the links because the model is a "skeletal" representation.

TABLE 1 Summary of quantitative measurements of clot parameters

Buffer	Link diameter*	Link length	Number of links per node
0.05 M	180 ± 42nm	1690 ± 1100nm‡	3.4 ± 0.8
0.20 M	70 ± 18nm	270 ± 160 nm‡	3.1 ± 0.3
0.40 M	39 ± 16nm	93 ± 42 nm§	3.1 ± 0.3

*Values for link diameter were measured from several images for each ionic condition.

‡Values for mean link length represent the sum of data from two different reconstructed clots.

§Values for mean link length were obtained by direct inspection from two-dimensional electron micrographs. A value of 540 ± 480 nm was obtained by three-dimensional reconstruction but did not include all links (see Discussion).

Appearance of three-dimensional images of fibrin clots at different ionic strengths

Any conclusions that arise from quantitative studies of any fibrous network are valid only if the specimens are well preserved and free from artifacts after preparation for microscopy. Critical point drying is a commonly used method that avoids many artifacts that occur with other techniques. However, traces of water or ethanol in the CO_2 during critical point drying causes fibrin fibers, as well as other fibrous structures, to appear unevenly thick and to form networks of tapering fibers, as a result of the fusion of fibers (Ris, 1985). This artifact is not present in our images (Fig. 1). Furthermore, the repeat of the fibrin band pattern, which is visible in some fibers in these images, is only 3% lower than that measured in x-ray fiber diffraction patterns of fully hydrated clots and negatively contrasted fibers, indicating that distortion is minimal.

Fibrin clots formed in 0.20 M saline buffer consisted of fiber bundles of relatively uniform size with very few extremely large or small bundles. Most large diameter links were bundles of average-sized fibers (60–80 nm). Very few free fiber ends and no unaggregated protofibrils were evident. Most of the clot branching junctions were areas where fibers intertwined and diverged and consisted of three links per branching junction. The overall appearance was of a mesh that is uniform in all three dimensions (Fig. 1 B).

In 0.40 M saline buffer, the majority of clot structures consisted of thin fibers with a few large fibers and fiber bundles (Fig. 1 C). The fibers appeared to be more densely packed than those in clots formed in 0.20 M saline buffer, with thinner fibers and considerably shorter distances between branching junctions. Often a meshwork of very fine fibers could be seen spanning the spaces between larger fibers. Although these fibers were readily visible in the original electron micrographs, the 1024 × 1280 pixel resolution of the monitor used for the image analysis system was insufficient to display these very fine fibers at the magnification used for these studies. As a result, the current method of link diameter measurement was not accurate for these very small fibers, but we estimated the diameter of these links to be considerably less than 10 nm, with some possibly being as small as protofibrils. A comparison of computer images and the original electron microscope negatives was made in order to determine the prevalence of these small fibers (see below). Limitations in the resolution of image digitization and the display of the computer system currently prevented accurate analysis of these fibers. Without the need to carry

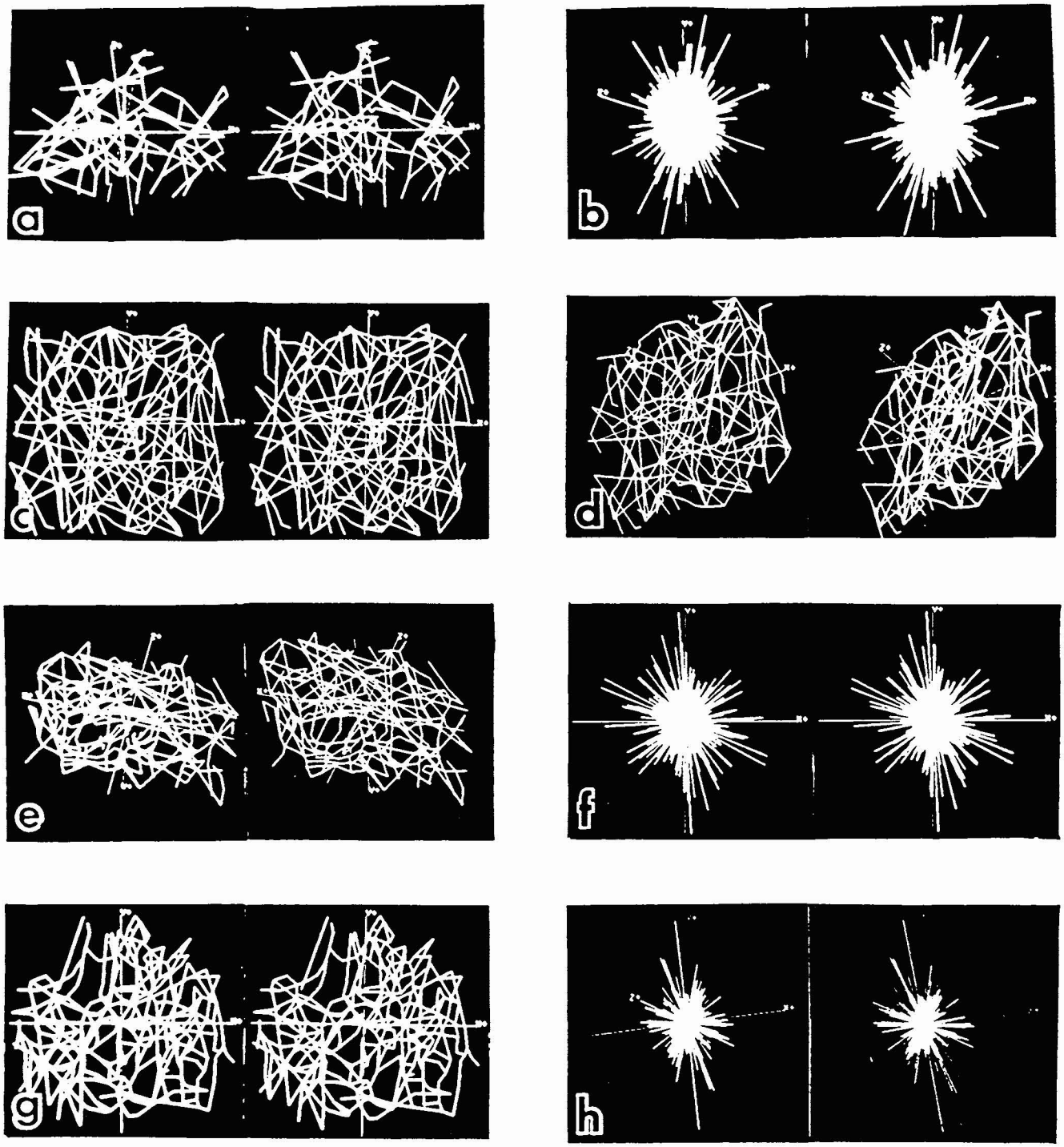

FIGURE 3 Three-dimensional models of IVEM clot images and alternate display of them as "sea-urchin" models (representation of spherical distribution of link lengths). In each case, stereo pairs are shown. (*A*) Three-dimensional model of clot formed in 0.05 M ionic strength buffer. (*B*) "Sea-urchin" model of clot formed in 0.05 M ionic strength buffer. (*C*) Three-dimensional model of clot formed in 0.20 M ionic strength buffer. (*D*), (*E*) Rotated views of the same three-dimensional model of clot formed in 0.20 M ionic strength buffer. (*F*) "Sea-urchin" model of clot formed in 0.20 M ionic strength buffer. (*G*) Three-dimensional model of clot formed in 0.40 M ionic strength buffer. (Note the limitations in the accuracy of this model described in the text.) (*H*) "Sea-urchin" model of clot formed in 0.40 M ionic strength buffer.

out analysis of the three different types of clots in the same way for ease of comparison, we could have digitized the images of clots at 0.4 M salt at higher resolution. The effect of the large number of these fibers on measurements of mean link length will be discussed below.

Clots formed in 0.05 M saline buffer exhibited very large diameter fiber bundles with occasional free truncated fiber ends and a larger variation in apparent link diameter (Fig. 1 A). Some free protofibrils were seen on the clot substrate. Generally, the clots formed in 0.05 M saline buffer were

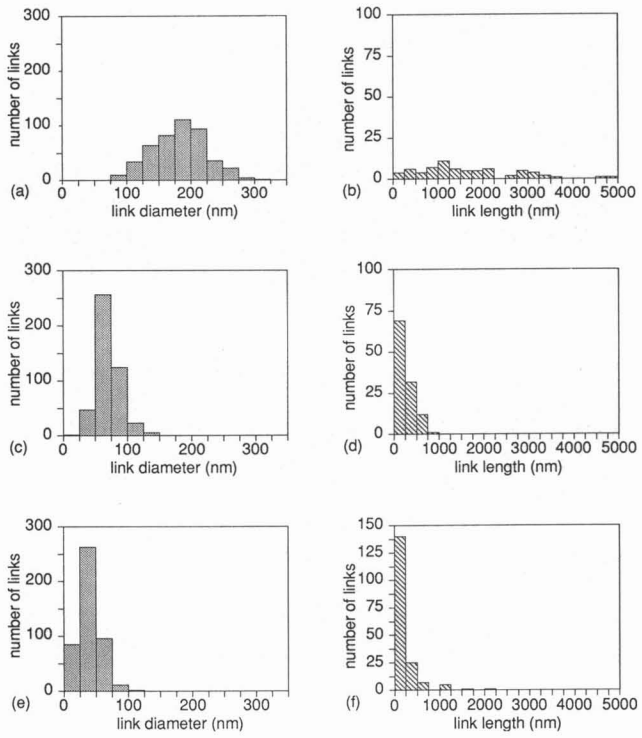

FIGURE 4 Histograms showing the size distribution of link diameters and link lengths derived from analysis of three-dimensional clot reconstructions under three different ionic conditions. Link diameter histograms are on the left, and the corresponding link length histograms are on the right. (*A*), (*B*) 0.05 M ionic strength buffer. (*C*), (*D*) 0.20 M ionic strength buffer. (*E*), (*F*) 0.40 M ionic strength buffer.

much less branched than clots formed in either of the two previous conditions. There were long distances where fibers were bundled parallel to each other with no branching junctions. The clot fiber bundles were widely spaced, with the result that the clot was very "porous," especially compared with high ionic strength clots. Most of the branching junctions were formed by the union of three links, but a few appeared to consist of more links (four or five). The appearance of more links per node may be a result of adjacent fiber bundles that would bring two or more branching junctions into close proximity.

Quantitative measurements of fiber networks

Electron micrographs were usually taken at a magnification of 10,000 or 30,000 times. The choice of magnification and pixel size in digitizing the images was a compromise between maximizing the number of branch points/links in the reconstruction (to obtain representative reconstructions and good averages) and the resolution. Usually micrographs taken at a magnification of 10,000× were digitized with a pixel size corresponding to ~3 nm. Examples of three-dimensional reconstructions of clots formed under each of the three different salt concentrations are shown in Fig. 3, *A*, *C*, *D*, *E*, and *G*. Many of the distinctive characteristics of these clots described in the last section can be more easily seen in these wire-frame models. Different views of the same network reveal new features of the structure (Fig. 3, *C–E*). The sea urchin plots give a direct visual impression of the relative lengths of the links and their orientations (Fig. 3, *B*, *F*, *H*). Furthermore, these plots demonstrate that there is no preferential orientation of the links in these clots and that the link lengths are similar in every direction. Thus, it may be concluded that these clots are homogeneous and are unlikely to have been flattened or deformed during specimen preparation. It is important to note that the fibers in thrombi or in clots formed in vivo may often have a preferential orientation that could be analyzed by using these sea urchin plots.

The distance between branching junctions in the fibrin clot, or mean link length, was the first parameter measured (Table 1). The distributions of link lengths for all ionic conditions are plotted in Fig. 4. Clots formed in 0.05 M saline buffer had the greatest mean link length, 1680 ± 1100 nm (mean ± SD), and the largest variation in link length, 200–5000 nm (Fig. 4 *B*). Clots formed in 0.20 M saline buffer exhibited link lengths with a mean of 270 ± 160 nm (Fig. 4 *D*). Statistical analysis by the unpaired *t*-test gave results of $p < 0.99$ for 0.05 M link length versus 0.20 M link length.

High ionic strength conditions (0.40 M) yielded fibers with a measured mean link length of 540 ± 480 nm (Fig. 4 *F*). However, the results of the high ionic strength clot analysis do not accurately reflect the clot structure under these conditions. These networks were made of so many thin fibers that a great many branching junctions and links were not included in the reconstructions. Detailed examination of the reconstructed models of the clots together with the stereo pairs of electron micrographs indicated that fewer than half of the branching junctions were included in the reconstruction. In addition, the numerous very fine fibers forming networks between larger diameter fibers were too small to be seen on the computer monitor. As a result, branching junctions were determined by inspection of stereo-pair electron micrographs and link lengths measured in two dimensions from photographic prints of electron micrographs, yielding values of 93 ± 42 nm. This method has inaccuracies that increase with the depth of the image, such that we can only estimate the average link length. Nevertheless, for clots formed at high ionic strength, direct measurement of link lengths is more accurate than using values from the computer reconstructions.

The average number of links per branching junction was also measured. Under all ionic conditions, the number of links from a particular branching junction was nearly always three (Table 1). Clots formed in 0.20 M and 0.40 M saline buffer were found to have an average of 3.1 ± 0.3 (mean ± SD) links at each branching junction. Low ionic strength clots (0.05 M) appeared to have a slightly larger proportion of branching junctions with four or five links. Clots formed in 0.05 M buffer were found to have an average of 3.4 ± 0.8 links at each branching junction. The tendency of fibers to form large fiber bundles under these ionic conditions made the discrimination between true branches and intertwined bundles difficult.

Calibrated photographic prints were made from electron micrographs of fibrin clots, and measurements were carried out so that the effects of the changes in ionic strength on link diameter could be determined. The results are summarized in Table 1. If the micrographs used were taken with IVEM, 0° tilt angle pictures were selected. Clots that were formed in low ionic strength buffer had the largest measured link diameters: in 0.05 M saline buffer, the mean clot link diameter was 180 ± 40 nm (mean ± SD). Clots that were formed in buffer close to physiological conditions (0.20 M) yielded links with a diameter of 70 ± 18 nm. Clots formed in high salt conditions, 0.4 M, had the smallest average link diameter, 39 ± 16 nm (Table 1).

The size distributions of fibrin link diameters for each clotting condition are plotted in Fig. 4. Clots formed in low ionic strength (0.05 M) exhibit mostly fiber bundles and few apparent individual fibers. The greatest range of link diameters, 75–300 nm, was found for clots formed in 0.05 M saline buffer (Fig. 4 *A*). Clots formed in 0.20 M saline buffer had link diameters of 30–130 nm (Fig. 4 *C*). Clots formed in 0.40 M saline buffer had a range of measured link diameters of 6–105 nm (Fig. 4 *E*). However, many of the structures in the micrographs were 6 nm or less in diameter and were not measured; these structures are probably individual protofibrils. The range of link diameters for 0.40 M and 0.20 M clots were very similar, approximately 100 nm, which was in sharp contrast to that of low salt fibers, whose link diameters varied by as much as 225 nm.

DISCUSSION

Observations of the fine structure of clots from whole blood plasma have been made since the early development of the electron microscope (Wolpers and Ruska, 1939). These investigations were enhanced by the development of purification techniques for human blood plasma proteins (Cohn et al., 1940, 1946). Hawn and Porter (1947) described the fibrin clot as "a tridimensional network of branching strands" in their experiments concerning the effect of pH on polymerization. These structures were found to be greatly affected by changes in the concentrations of fibrinogen and thrombin, the temperature, pH, and ionic strength of the polymerizing buffer and other biochemical factors (Ferry and Morrison, 1947).

The effects of such factors on clot structure have been observed by scanning electron microscopy (Langer et al., 1988; Weisel and Nagaswami, 1992; Dang et al., 1989). This technique is excellent for visualization of differences in structure; the appearance of clots formed under various conditions is strikingly different. However, both the resolution and the ability to visualize deeper structures are limited. In contrast, high resolution transmission electron microscopy has been used to examine fibrinogen and fibrin monomers, protofibrils and fibrin fibers, but its usage for whole clots is limited by the thickness of the specimens. Higher accelerating voltages allow thicker specimens to be visualized, which avoids many of the artifacts, such as stretching or syneresis, that are seen in thin-film preparations. High-voltage transmission electron microscopy has been used to examine very thin specimens of fibrin clots (Mosesson et al., 1987; Müller et al., 1984) in which branching junctions were identified through enhancement of depth perception by the use of stereo pairs. However, most clots are far too complex to be comprehended by simple visual inspection. For further study, it is necessary to transform the complex networks into simpler wire-frame representations and characterize them quantitatively.

For experiments described in this paper, we have used conventional stereo pairs to visualize several types of clot, including those formed under physiological conditions, and have developed new methods for analyzing clot networks quantitatively. There are many advantages to be gained by analyzing the clot structures through the combined use of stereo-pair visualization and computer analysis of images from the intermediate voltage electron microscope. These images are of higher resolution than those obtained from scanning electron microscope specimens, allowing more details of fibrin fiber branching and associations to be seen. The metal vapor coating (12–14 nm) required for conventional scanning electron microscope specimens is eliminated, allowing more accurate measurements of link diameters and the ability to observe very small fibers and protofibril structures that would otherwise be obscured. Using IVEM to examine specimens permits high resolution imaging without features deep within the structure being obscured. The greater penetration arising from the use of higher accelerating voltages allows visualization of the entire clot rather than only the surface features. In addition, thermal damage that occurs to the specimens, especially clots formed in 0.4 M NaCl, during observation in a conventional transmission electron microscope was largely prevented by a light coating of carbon and carrying out the microscopy at 400 kV.

Fibrin clots are by nature three-dimensional networks that serve to span and fill damaged areas of vascular tissue by their attachment to adjacent cell membranes. The mechanisms and kinetics of polymerization have an important role in determining the structural relationships of fibers. The use of stereo pairs has several inherent advantages when one is analyzing networks. A single fiber may be observed along its entire length to determine the number and type of associations with other clot structures. With stereo pairs it becomes possible to distinguish true branching junctions from fibers that cross each other at different depths. In conjunction with computer analysis techniques, the distances between clot fiber branching junctions (link length) can be measured accurately, and clot link diameter and angular orientation can also be determined.

By tracing fibrin fibers, it is possible to reconstruct the clot as a three-dimensional "wire-frame" model. This model may be viewed concurrently with the digitized stereo pair used for image analysis. Models may be rotated 360° on any axis, providing viewpoints that cannot be obtained by direct observation of the specimen itself. A lateral view, for example (Fig. 2 *E*), can provide a simple and qualitative basis for

comparing the distribution of fibers in the z direction, especially between models derived from clots formed under different ionic conditions. Even a slight rotation can allow the observation of a structure that is obscured by other fibers. It is also possible to "zoom" the wire-frame model for closer inspection of details. The growing model can be edited while the clot network is being traced, to correct obvious errors and to detect anomalies in the clot structure. Individual branching junctions and connecting links can be identified for correlation with stereo-pair images. A second type of model was developed in addition to the Cartesian coordinate wire-frame model. By translating the end of a fiber segment to the origin while preserving its angular orientation, a model is produced that resembles a sea urchin. The relative length, density, and angular orientation of fibrin links from different clot conditions can readily be compared with this view.

Clots that were polymerized in 0.20 M saline buffer form a uniform mesh in three dimensions. There was no obvious change in structure with a change in the depth or orientation of the observed area. The fibers and fiber bundles were of a uniform size, with very few free ends, and no protofibrils were visible in these preparations. Branching structures were regularly spaced in all dimensions. Clots that were polymerized in 0.40 M saline buffer appeared more fragile and less ordered. The fibers were variable in diameter and highly branched. Numerous protofibrils and small fibers could be seen on the grid surface; apparently these were structures that had not been incorporated into the clot at the time of fixation. Very small fibers (5–15 nm) can be seen spanning networks of larger fibers. The clots formed in low salt buffer conditions (0.05 M) were also significantly different in appearance. The fiber bundles had a much greater diameter, and free fiber ends were occasionally seen. There were large areas of open space bounded by the very large fiber bundles, so that the clot was very "porous."

The diameter of fibrin fibers and fiber bundles are the result of several kinetic processes that occur concurrently; these include fibrinopeptide release, protofibril formation and association, and lateral aggregation of fibrin fibers to form bundles (Weisel and Nagaswami, 1992). Small variations in link diameter may be attributed to differences in clot fixation and dehydration and in the method used for actual measurement. For example, link diameter measurements here tend to be slightly less than those obtained by measuring negatively contrasted fibers, most likely because of shrinkage from critical-point drying. Other differences in methods of preparation may also cause variations; e.g. scanning electron microscope specimens generally require the use of a metal vapor coating, and therefore measurements of link diameter from their images tend to yield slightly larger values than those obtained from transmission electron microscopy images.

While individual fiber diameters remain fairly constant (≈50–100 nm) under a wide range of conditions, lateral aggregation of fibers themselves can vary widely, resulting in links of varying diameters (Weisel, 1986). For the sake of consistency, we use the term "link diameter" because the links between branching junctions may consist of either fibers or fiber bundles, depending on the conditions of clot formation. The range of link diameters for clots formed in high ionic strength buffer (0.40 M) was approximately 23–55 nm (Table 1). Inasmuch as link diameter represents a balance between protofibril extension and lateral aggregation, the high ionic strength environment appears to inhibit the lateral aggregation of protofibrils and fibers, and the result is narrower diameter links and shorter connecting links between branching junctions. The opposite of this effect is apparent in the case of clots formed in the low ionic strength buffer, where the link diameter ranges from 140 to 220 nm and their link lengths are 600–2800 nm (Table 1).

In general, an increase in the ionic strength of the clotting buffer resulted in a decrease of the mean link length. The greatest separation of branching junctions, 1690 ± 1100 nm, was found in clots formed in 0.05 M saline buffer, while clots formed in 0.20 M saline buffer had branching junctions separated by 270 ± 160 nm. For clots formed in 0.40 M saline buffer, the link diameter was the smallest of that in all three ionic conditions, but the link length was difficult to measure. A mean link length of 540 ± 480 nm was obtained by computer reconstruction and modeling, but this value was not accurate because of the complexity of the networks and the small fiber sizes. Stereo-pair electron micrographs were used to determine branching junctions, and two-dimensional measurements were made on photographic enlargements of electron micrographs. With these data we determined the mean link length to be 93 ± 42 nm for 0.40 M clots.

The method of measuring link length directly from electron micrographs is limited to giving the projected length only, while the link lengths determined from the computer reconstructions are real lengths. In these experiments, we were concerned with the comparison of clots formed under different ionic environments and chose digitizing conditions accordingly. Future detailed reconstructions and analysis of very complex networks, such as those clots formed in 0.40 M salt, would require micrographs taken at higher magnifications and reconstruction of smaller areas. We are also in the process of developing computer algorithms that would automate the network tracing process, allowing networks that are too complex for manual inspection to be analyzed and reconstructed.

There is a potential error in z-axis determinations that can result from the small stereo separation (tilt angle). If we assume that the cursor error is Dx, then x measurements are uncertain by a factor of Dx, and the uncertainty in z (Dz) is given by $Dz = Dx/\sin\theta$, where θ is one-half the angle between the two views of the stereo pair. By repeated measurements, the placement error was determined to be approximately 2 nm in the x-y plane. Thus, the placement error is ~10% of the link length in the z axis. However, few fibers are oriented solely along the z axis, and the error decreases with orientation away from the z axis. The figure of 10% is also dependent on the precision of tilt angle measurement,

with larger tilt angles yielding a more accurate estimate. This error can be corrected by analyzing several stereo pairs at different tilt angles, which will be carried out in future investigations. It will be possible to construct a better three-dimensional, rotatable image of a clot by combining stereo-pair images taken at varying tilt angles to increase the accuracy in the z direction.

It has been demonstrated that there is a relationship between clotting time and the pore size in clots; it appears that a framework is laid down that can be added to after the gel point (Hantgan and Hermans, 1979; Blombäck and Masahisa, 1982). We have shown that there also appears to be a relationship between link diameter and mean link length: a decrease in ionic strength of the clotting buffer below normal physiological levels results in increased link diameter and mean link length. Conversely, an increase in ionic strength of the clotting buffer above normal physiological levels appears to result in decreased link diameter and mean link length.

One of the most striking observations from these experiments is the consistency in the number of branches that are found at a fiber branching junction. Clots formed under any of the ionic conditions used here (0.05 M, 0.20 M, 0.40 M) typically have simple branching configurations, with a total of three branches at each node. While this is not an inviolable rule and branching junctions with 4–5 branches are seen occasionally, the majority of clots structures formed in 0.20 M saline buffer have three branches per branching junction. Clots formed in low salt (0.05 M) have far fewer branching junctions owing to increased link length and link diameter, but the majority of nodes still have three branches. Note that the fibrin clot is very different in this respect from the clot in many other polymer networks, such as lightly cross-linked rubbers, in which four strands usually radiate from each node (Ferry, 1980).

Previous confocal light microscopy studies have visualized nodes, often with more than three fiber bundles apparently protruding from each (Blombäck et al., 1989). Confocal microscopy allows the examination of optical sections of hydrated clots and provides evidence on clot structure complementary to that from electron microscopy. Our results clarify the nature of these nodes and demonstrate that most branch points consist of three links each. Thus, it appears that the structures observed by confocal microscopy are more complex and probably represent trifunctional branch points with other fibers nearby that cannot be distinguished with an optical resolution of approximately 0.25 μm and the 1 μm thick optical sections used for those experiments.

The observation that most branching junctions consist of three links and that the link length is directly related to the degree of lateral aggregation of protofibrils and fibers into fiber bundles suggests a simple mechanism for branching. A branching junction consisting of three links is likely to be a point at which two parallel strands of a growing clot network diverge from each other. Depending upon the stage of assembly, these strands may be fiber bundles, fibers, protofibrils, or even individual filaments of a protofibril. For example, two fibers that are bound together or intertwined will diverge at some point, because fibers are very long, and, in fact, it is rare to see a fiber end under any of the ionic conditions used in these experiments. Thus, fibers must merge with each other and later diverge again. With an increasing extent of lateral aggregation, adjacent fibers may bind or intertwine over greater lengths. Therefore, the distance between branching junctions would increase as observed. Conversely, at high salt concentrations, where there is little lateral aggregation, fibers may bind or intertwine only over shorter distances; therefore, the distance between branching junctions in these clots is small. In other words, there may be nothing unique about these branching junctions. It appears that they are simply a reflection of the extent of lateral aggregation of protofibrils and fibers combined with the fact that long fibers merge and separate.

Study of the final clot structures cannot be used to derive a detailed molecular mechanism of branching, but the reasoning proposed here is consistent with ideas that have been presented previously. Hantgan and Hermans (1979), using data from light scattering and mechanical testing, found that the gel point was reached well before the clot exhibited its maximal degree of light scattering and its maximum rigidity. They proposed that the basic "skeleton" of the clot is formed by the time the gel point is reached and that subsequent lateral associations between fibers (binding or intertwining) and addition of protofibrils to existing fibers adds to the rigidity of the clot. Further experiments in which light scattering data were correlated with electron microscope images showed that high ionic strength limited both the rate and the extent of lateral aggregation of fibers (Hantgan et al., 1980). Molecular mechanisms for branching have also been suggested by Mosesson et al., who observed branching junctions at high ionic strength consisting of three links, each with a diameter and mass corresponding to a single protofibril (Mosesson et al., 1989; Mosesson and DiOrio, 1993). These junctions, called "trimolecular" branching points, would be generated very early during the stage of protofibril formation.

The relationship between lateral aggregation and branching described here has important consequences for the mechanical properties of clots. In accordance with observations, clots formed under high salt concentrations with little lateral aggregation and many branching junctions are highly elastic, although perhaps more fragile. In contrast, those formed under low salt concentrations, with very thick fiber bundles and widely spaced branching junctions, are much more viscous and collapse easily.

Quantitative analysis of clot structures formed from naturally occurring and recombinant fibrinogen variants may lead to a greater understanding of the biochemical and structural properties of fibrin clots and molecular mechanisms of assembly. These studies could have important implications for developing clinical antithrombotic and hemostatic agents. At the present time, most of the working hypotheses have been

based on qualitative assessments of the visual appearance of the clot and correlations with biochemical data.

With the software described in this paper, such qualitative information about biological networks can now be supplemented with three-dimensional reconstructions and determination of network parameters. Our computer-assisted system of analysis is capable of providing quantitative data that could be applicable to the study of many other biological structures that have fibrous or reticular elements. Some possible areas for modeling and analysis are neural networks and neurofibrillar structures, as well as cytoskeletal components such as microtubules, microfilaments, and intermediate filaments. Components of the extracellular matrix are another possible area of application. Investigation of such networks using these methods may lead to a greater understanding of their biological properties and functions.

We thank Dr. Jose A. Martinez (Thomas Jefferson University, Philadelphia) for providing purified human fibrinogen and Mr. Christian Haselgrove for the development of the three-dimensional model display and analysis software. We acknowledge the support of National Institutes of Health (NIH) grants HL 30954 (J.W.W.) and RR 2483 (Dr. Lee D. Peachey, NIH Intermediate Voltage Electron Microscope Biomedical Image Analysis Resource, Department of Biology, University of Pennsylvania) and thank Dr. Peachey for advice and support.

REFERENCES

Blombäck, B., K. Carlsson, B. Hessel, A. Liljeborg, R. Procyk, and N. Aslund. 1989. Native fibrin gel networks observed by 3D microscopy, permeation and turbidity. *Biochim. Biophys. Acta.* 997:96–110.

Blombäck, B., and O. Masahisa. 1982. Fibrin gel structure and clotting time. *Thromb. Res.* 25:51–70.

Carr, M. J., D. A. Gabriel, and J. McDonagh. 1986. Influence of Ca^{2+} on the structure of reptilase-derived and thrombin-derived fibrin gels. *Biochem. J.* 239:513–516.

Cohn, E. J., M. L. McMeekin, J. L. Oncley, J. M. Newell, and W. L. Hughes. 1940. Preparation and properties of serum and plasma proteins, Part III. *J. Am. Chem. Soc.* 62:3396–3401.

Cohn, E. J., L. E. Strong, W. L. Hughes, Jr., D. J. Mulford, J. N. Ashworth, M. Melin, and H. L. Taylor. 1946. Preparation and properties of serum and plasma proteins, Part IV. *J. Am. Chem. Soc.* 68:459–467.

Dang, C. V., C. K. Shin, W. R. Bell, C. Nagaswami, and J. W. Weisel. 1989. Fibrinogen sialic acid residues are low affinity calcium-binding sites that influence fibrin assembly. *J. Biol. Chem.* 264:15104–15108.

Erickson, H. P., and W. E. Fowler. 1983. Electron microscopy of fibrinogen, its plasmic fragments and small polymers. *Ann. N. Y. Acad. Sci.* 408: 146–163.

Ferry, J. D. 1980. Viscoelastic Properties of Polymers. John Wiley & Son, New York.

Ferry, J. D., and P. R. Morrison. 1947. Preparation and properties of serum and plasma proteins. VIII. The conversion of human fibrinogen to fibrin under various conditions. *J. Am. Chem. Soc.* 69:388–400.

Fowler, W. E., R. R. Hantgan, J. Hermans, and H. P. Erickson. 1981. Structure of the fibrin protofibril. *Proc. Natl. Acad. Sci. USA.* 78:4872–4876.

Hantgan, R., W. Fowler, H. Erickson, and J. Hermans. 1980. Fibrin assembly: a comparison of electron microscopic and light scattering results. *Thromb. Haemost.* 44:119–124.

Hantgan, R. R., and J. Hermans. 1979. Assembly of fibrin: a light scattering study. *J. Biol. Chem.* 254:11272–11281.

Hardy, J. J., N. A. Carrell, and J. McDonagh. 1983. Calcium ion functions in fibrinogen conversion to fibrin. *Ann. N. Y. Acad. Sci.* 408:279–287.

Hawn, C. V. Z., and K. R. Porter. 1947. The fine structure of clots formed from purified bovine fibrinogen and thrombin: a study with the electron microscope. *J. Exp. Med.* 86:285–296.

Langer, B. G., J. W. Weisel, P. A. Dinauer, C. Nagaswami, and W. R. Bell. 1988. Deglycosylation of fibrinogen accelerates polymerization and increases lateral aggregation of fibrin fibers. *J. Biol. Chem.* 263: 15056–15063.

Latallo, Z. S., A. P. Fletcher, N. Alkjaersig, and S. Sherry. 1962. Inhibition of fibrin polymerization by fibrinogen proteolysis products. *Am. J. Physiol.* 202:681–686.

Medved', L., T. Ugarova, Y. Veklich, N. Lukinova, and J. Weisel. 1990. Electron microscope investigation of the early stages of fibrin assembly. Twisted protofibrils and fibers. *J. Mol. Biol.* 216:503–509.

Mosesson, M. W., J. P. DiOrio, M. F. Müller, J. R. Shainoff, K. R. Siebenlist, D. L. Amrani, G. A. Homandberg, J. Soria, C. Soria, and M. Samama. 1987. Studies on the ultrastructure of fibrin lacking fibrinopeptide B (beta-fibrin). *Blood.* 69:1073–1081.

Mosesson, M. W., and J. P. DiOrio. 1993. Evidence for a second type of fibril branch point in fibrin polymer networks, the trimolecular junction. *Blood* 82:1517–1521.

Mosesson, M. W., K. R. Siebenlist, D. L. Amrani, and J. P. DiOrio. 1989. Identification of covalently linked trimeric and tetrameric D domains in crosslinked fibrin. *Proc. Natl. Acad. Sci. USA.* 86:1113–1117.

Müller, M. F., H. Ris, and J. D. Ferry. 1984. Electron microscopy of fine fibrin clots and fine and coarse fibrin films. *J. Mol. Biol.* 174:369–385.

Ris, H. 1985. The cytoplasmic filament system in critical point-dried whole mounts and plastic embedded sections. *J. Cell Biol.* 100:1474–1487.

Weisel, J. W. 1986. Fibrin assembly. Lateral aggregation and the role of the two pairs of fibrinopeptides. *Biophys. J.* 50:1079–1093.

Weisel, J. W., and C. Nagaswami. 1992. Computer modeling of fibrin polymerization kinetics correlated with electron microscope and turbidity observations: clot structure and assembly are kinetically controlled. *Biophys. J.* 63:111–128.

Weisel, J. W., C. Nagaswami, and L. Makowski. 1987. Twisting of fibrin fibers limits their radial growth. *Proc. Natl. Acad. Sci. USA.* 84:8991–8995.

Wolpers, C., and H. Ruska. 1939. Strukturuntersuchungen zur Blutgerinnung. *Klin. Wochnschr.* 18:1111–1116.